Taylor & Francis
Taylor & Francis Group

Desalination and Water Treatment

ISSN: 1944-3994 (Print) 1944-3986 (Online) Journal homepage: http://www.tandfonline.com/loi/tdwt20

Landuse and NDVI change analysis of Sperchios river basin (Greece) with different spatial resolution sensor data by Landsat/MSS/TM and OLI

Vassiliki Markogianni & Elias Dimitriou

Desalination and Water Treatment
www.deswater.com

(2016) 1–12

doi: 10.1080/19443994.2016.1188734

Landuse and NDVI change analysis of Sperchios river basin (Greece) with different spatial resolution sensor data by Landsat/MSS/TM and OLI

Vassiliki Markogianni*, Elias Dimitriou

Institute of Marine Biological Resources and Inland Waters, Hellenic Centre for Marine Research-H.C.M.R., Anavissos 19013, Greece, Tel. +30 22910 76349; Fax: +30 2291076419; email: vmarkogianni@hcmr.gr (V. Markogianni), Tel. +30 22910 76389; Fax: +30 2291076419; email: elias@hcmr.gr (E. Dimitriou)

Received 7 March 2016; Accepted 29 April 2016

ABSTRACT

The assessment of land use–land cover (LULC) and normalized difference vegetation index (NDVI) changes on hydrology is essential for the development of sustainable water resource strategies. This study focuses on Sperchios river catchment, a complex and very heterogeneous area made up of numerous land covers that are difficult to map due to spectral similarities. Difficulties such as multi-seasonal spectral variables corresponding to different stages of land cover phenological development were addressed by choosing an unsupervised classification algorithm called k-means in combination with the Corine land cover database and past scientific studies. Available remote sensing data included three Landsat images (MSS, TM, OLI) all of which were resampled to a common 30-m resolution. Final LULC classifications in the period 1972–2013 separated forest, agricultural land and heath land and detected unified bare with urban land and pastures with areas of low vegetation. The recorded results include a significant reduction (–80%) of vegetation (NDVI values), 28 and 26% reduction rates in forests and pastures-low vegetation, respectively, a strong increase (114%) in heath land and an 47% increase, as concerns the agricultural land. Using of random points estimated the classification accuracy to be 75.4 and 85.2% for LULC of 1972–2013, respectively. This particular study constitutes a preliminary stage of an attempted integrated basin management of Sperchios river intending to contribute to overall ecological quality assessment of Sperchios river.

Keywords: LULC; NDVI; Landsat/MSS/TM/OLI; Sperchios river

1. Introduction

In recent times, remote sensing has been evolved into a predominant tool for environmental monitoring, global climate comprehension and amplification of advancing and generative activities in a specific district. Satellite remote sensing is used with great success in monitoring and detection of vegetation and land cover changes. Vegetation indices, established on remotely sensed spectral reflectance in the near-infrared and visible channels, have been extensively employed for monitoring vegetation cover, health status and Eco systemic diversities [1–5]. They have been utilized to support land use mapping and change

*Corresponding author.

Presented at the 5th International Conference on Environmental Management, Engineering, Planning and Economics (CEMEPE) 14–18 June 2015, Mykonos, Greece

detection [6–10]. Among many vegetation indices normalized difference vegetation index (NDVI) has been most regularly used for vegetation monitoring in various studies [11–18]. Furthermore, variety in the superficial vegetation influence the equilibrium of local ecosystems, research on the vegetation heterogeneity is the substructure of the ecological conservation [19,20].

NDVI nominates the growth condition of vegetation while performs as an effective index for monitoring vegetation fluctuations [21].

Furthermore, remote sensing has long been an efficient expedient of monitoring land cover with its immediate capacity to compile data at large scale, and is developed into a compelling practice to retrieve forest cover information [22,23].

Resolutions of Landsat remote sensing data (30 m) are fundamental for land use and land cover mapping and change detection due to anthropogenic factors usually at a small scale [23]. Present Landsat resolution land cover maps are usually resulted from supervised or unsupervised classification of single Landsat bands [4,24–26].

Land use changes are the dominant reason provoking habitat deterioration and water quality degradation [27–29]. Natural mechanisms and issues of human activities are major reasons of land use change [30,31]. Evolution activities such as agriculture, urbanisation, forestry and industries favour more intensive land use which expands runoffs and the transfer of pollutants directly into the adjacent rivers, streams and sea [32–34]. Their water quality is influenced by human activities through point source pollution, such as wastewater treatment facilities and non-point source pollution, such as runoff from urban areas, mining and farmlands [35,36]. Urbanization maximizes the environmental problems concerning soil deterioration with significant effects on water quality [37].

While previous studies have evaluated the agreement in surface reflectance and vegetation indices derived from multiple sensors, mainly focusing on Landsat TM/ETM+ and MODIS instruments [38–40], this study examines the characteristics of the NDVI and land uses derived from the newly launched Landsat 8 OLI sensor and combines them with the respective ones derived from Landsat MSS and TM. This particular effort has been conducted within the framework of the KRIPIS research project which is oriented towards the development of methodologies for integrated river basin management and associated coastal and marine zone with study areas the Sperchios river and Maliakos Gulf (Greece) and constitutes a preliminary stage intending to contribute to overall ecological quality assessment of Sperchios river.

2. Methodology

2.1. Study area

Sperchios river and its deltaic system is located in Central Greece and it has been included in the NATURA 2000 network with code GR2440002, where anthropogenic interventions in the delta area, especially after the 1950s [41 in 42], has influenced its natural habitats each one on a different degree, depending on the kind, the size and the location of the intervention.

River Sperchios is 85 km long and the total area of its drainage basin is 1,907.2 Km^2 [43 in 42], Fig. 1. It springs from Timfristos (2,312 m), Vardousia, Orthris, Oiti and Kallidromo and empties in Maliakos gulf, where its delta is formed. In the area of embouchure, the main river bed divides into three new beds, the old bed, the newer bed and the diversion bed. Within the drainage basin, steep slopes are dominant and for the total area the average slope is 33%. The river Spercheios Delta occupies an area of 196 Km^2 and extents about 4 km east of Anthili village and south-east of Lamia city. The climate in the area of the Sperchios drainage basin belongs to the sub-tropical Mediterranean zone, with warm and dry summer and mild and wet winter [42].

Furthermore, the "riparian tree vegetation: consist of willows, white poplars, planes, alders, mainly along the river bank, in mixed and pure stands. The riparian forest in the upper part of the delta occupies extended areas with width a ranging from few up to several hundred meters. The greatest part of the riparian forest is found in the upper part of the river (from Makrakomi to Messopotamia)" [41 in 42].

The Delta and the lowland sedimentary area of river Sperchios, geologically consist of quaternary depositions and specifically clays, sand, pebbles gravels which compose a gentle to flat landscape (slope 0–15%), on which the cultivated agricultural areas extent as well the deltaic marshes and tidal area. It contributes significant amounts of brought materials in the lower area of discharge, due to the presence of erosion prone flysch in its basin. These materials deposit and enrich the plane of Lamia and the Delta [44 in 42]. Changes in sediment transport, geomorphological evolution of Sperchios river delta, mainly due to human activities, climate changes and the action of the storm waves have been observed [45 in 42].

Finally, lowland areas have been created from the transport and deposition of suspended particulate matter from the river [42].

2.2. Satellite imagery and preprocessing elaboration

In this study, vegetation and land cover detection at a catchment level was initially implemented by

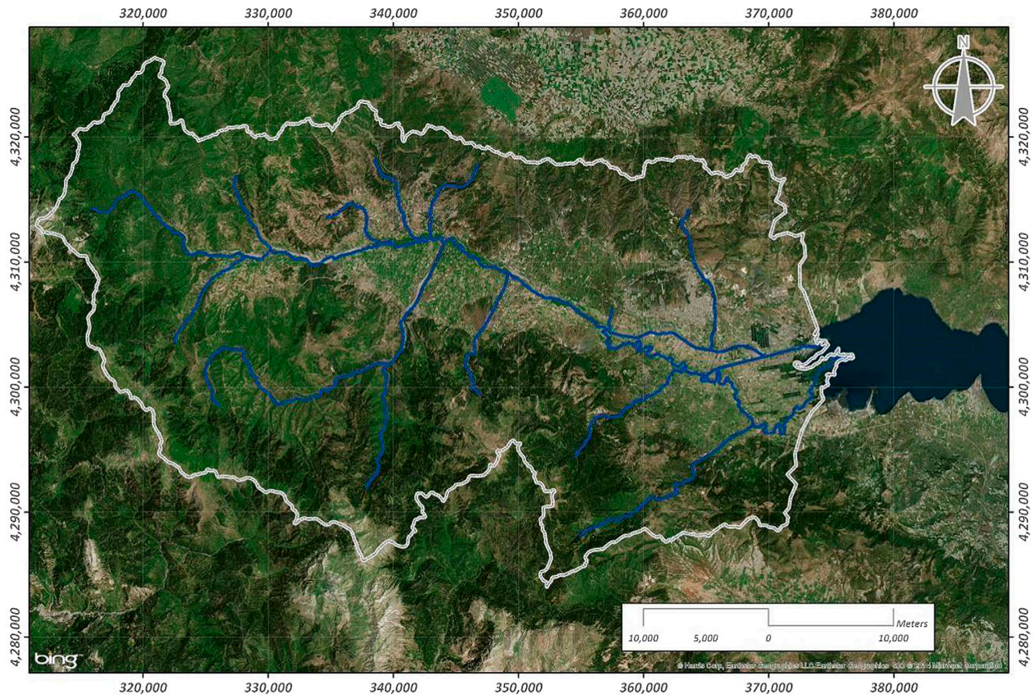

Fig. 1. Sperchios river’s basin and Maliakos Gulf.

calculating NDVI. For this purpose, satellite imagery from different remote sensors was used (Landsat MSS, TM, OLI) to generate vegetation and land cover maps. The satellite images were acquired from the USGS Data Centre (United States Geological Survey) and the acquisition dates are 08/09/1972 (Landsat 1 MSS), 08/06/1984 (Landsat 5 TM) and 12/09/2013 (Landsat 8 OLI).

The data elaboration and analysis were conducted in ESRI’s ArcGIS 10.1 software, while for the analysis of the satellite imagery, the ENVI 5.1 software was used. After selecting the study area scenes the digital data were initially resampled to a common 30 m resolution, subsequently were georeferenced and geographically converted from WGS84 to EGSA87 coordinate system (National Datum) and ultimately were submitted to the following procedures:

(1) Geometric correction (using GCP).
(2) Radiometric correction for the conversion of actual radiance values.

The formula used for this purpose is [Eq. (1), 46]:

$$L_{\lambda} = \{(L_{\mathrm{MAX}\lambda} - L_{\mathrm{MIN}\lambda})/(Q_{\mathrm{CALMAX}} - Q_{\mathrm{CALMIN}})\} \times (Q_{\mathrm{CAL}} - Q_{\mathrm{CALMIN}}) + L_{\mathrm{MIN}\lambda} \tag{1}$$

where L_{λ} is the cell value as radiance, Q_{CAL} is the digital number, $L_{\mathrm{MIN}\lambda}$ is spectral radiance scales to Q_{CALMIN}, $L_{\mathrm{MAX}\lambda}$ is spectral radiance scales to Q_{CALMAX}, Q_{CALMIN} is the minimum quantized calibrated pixel value and Q_{CALMAX} is the maximum quantized calibrated pixel value:

(3) Atmospheric correction (dark object subtraction technique) was also applied on the images through the darkest-pixel subtraction technique [47,48] via the relevant ENVI software tool.

2.3. NDVI

We used the following equation to estimate NDVI [Eq. (2), 49]:

$$\mathrm{NDVI} = (\mathrm{NIR} - R)/(\mathrm{NIR} + R) \tag{2}$$

where NIR and R are the reflectance radiated in the near-infrared wave band (4) and the visible red (3) wave band of the satellite TM radiometer, respectively. Regarding the Landsat 1 MSS sensor, the NIR band is the 7 (0.8–1.1 μm) and the red the 5 (0.6–0.7 μm) wavebands, respectively, and the NIR and red bands of Landsat 8 OLI are the 5 (0.85–0.88 μm) and the 4 (0.64–0.67 μm), respectively.

This estimation was implemented for each image with ENVI 5.1 software and the resulting raster files were imported into ArcGIS 10.1 for further processing and statistical analysis. Each raster had a cell size of 30 m. The estimation in this approach generated three NDVI maps (with the same cell size) for the aforementioned dates in a raster format. The changes in NDVI between 1972 and 2013 were estimated using the following widely used mathematical equation (Eq. (3)):

$$\% \text{ NDVI change} = 100 \times (\text{NDVI}_{2013} - \text{NDVI}_{1972})/\text{NDVI}_{1972} \quad (3)$$

2.4. Land uses

The *k*-means unsupervised classification algorithm [50–52] was used to detect the various land cover types in the study area and the results were compared with recent land use maps Corine 2000 database (COoRdination of INformation on the Environment) and available land use maps of Sperchios river basin from another scientific study [53].

The *k*-means classification algorithm is based on a cluster analysis method, aiming to partition n observations into *k* clusters in which each observation belongs to the cluster with the nearest mean. This process was repeated by altering the number of classes until the control points were accurately classified according to the aforementioned supplementary data (Corine land cover 2000 data base and available land use maps). The classification algorithm was first applied to the most recent image (Landsat eight, September 2013) since this offered the opportunity to use all of the available land cover information for validation (Corine data base and Google Earth). The same process followed for September 1972 using as exemplar the classification of 2013. The *k*-means classification algorithm was selected after several test runs with the available imagery and comparison with the results provided by other commonly used algorithms such as the Iterative Self-Organizing Data Analysis Technique (ISODATA).

The classification results included the following categories: forest, agricultural land, heath land, unified bare with urban land and unified pastures with areas of low vegetation. Moreover, in order to quantify each classification errors, 200 random points were created, through the common ArcGis tool, inside different land uses of each imagery. Creating random points is widely used concerning the classification accuracy assessment [54]. In the following, visual checks were carried out in order to estimate the percentage agreement with the respective remotely sensed land uses.

3. Results

3.1. NDVI mapping

The NDVI map of 1972 presents values ranging from –0.01 to almost 0.6 (Table 1, Fig. 6), while the mean NDVI value of the whole catchment is 0.21 (Figs. 2 and 6). The spatial distribution of the vegetation is characterized by dense, growing vegetation in regions with medium and high elevation (500–1,400 m) and sparse or annual vegetation types in lowland regions (0–230 m) where bare-urban land and pastures are detected.

In the 1984 vegetation map, the mean NDVI value reaches 0.3, while the spatial pattern of the maximum and minimum values is similar to that of the 1972 vegetation map (Table 1, Figs. 3 and 6).

The NDVI values of 2013 range from –0.16 to 0.4 and the mean NDVI value is 0.04 (Table 1, Figs. 4 and 6).

From the aforementioned results, it becomes obvious that the vegetation of 1972–1984 is denser and healthier compared to the vegetation of 2013, mainly in regions that are dominated by forests. This fact can also be ascertained by the mean NDVI values of each date and the frequency distribution of NDVI values of each year (Figs. 5 and 6). The majority of NDVI values of 1972–1984 are distributed above the zero point whereas a high percentage of NDVI values of 2013 are negative (negligible vegetation). Even though data distribution of 1972–2013 tend to resemble to a normal one, only the median value of 1972 data is almost in the middle of the distribution skeleton. Moreover, skewness of 1984 data is equal to –0.39 (Table 1, Fig. 5). Furthermore, extreme negative values are

Table 1
Descriptive statistics and frequency distribution table of NDVI values in 1972, 1984, and 2013

		1972	1984	2013
Min.		−0.01	−0.12	−0.16
Max.		0.56	0.73	0.39
Average		0.21	0.31	0.04
Standard Deviation		0.1	0.17	0.1
N	Valid	18,455	18,452	18,460
	Missing	11	14	6
Median		20,664	32,894	03,861
Skewness		176	–385	155
Std. error of skewness		018	018	018
Kurtosis		–366	–289	189
Std. error of kurtosis		036	036	036
Percentiles	25	13,977	20,389	–01,549
	75	27,967	43,552	09,863

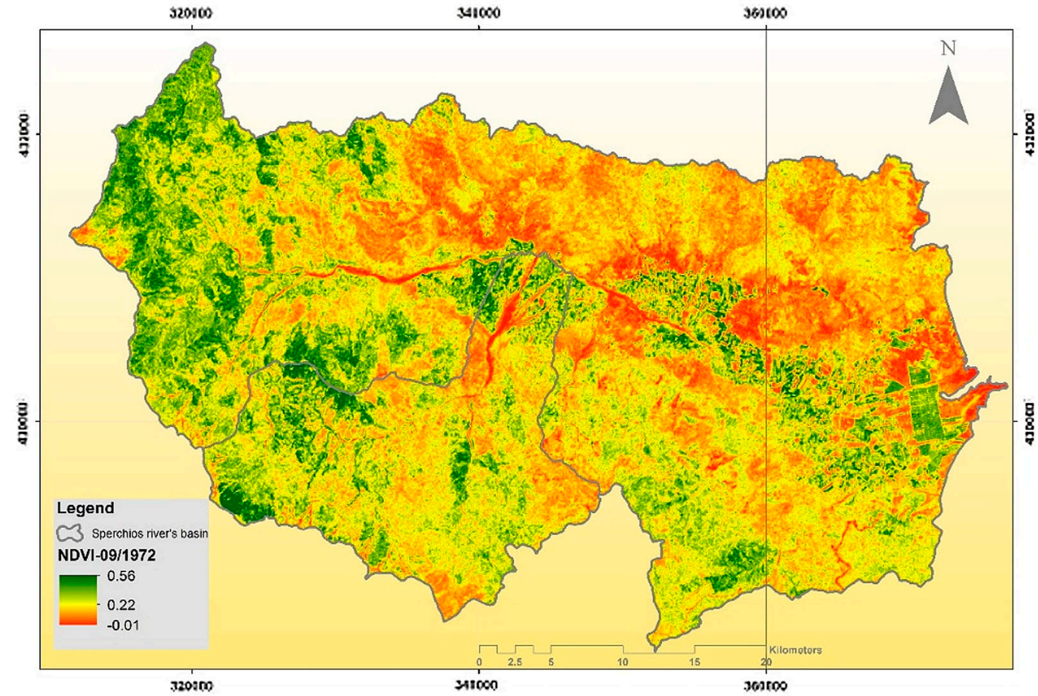

Fig. 2. NDVI of Sperchios river's basin in 1972.

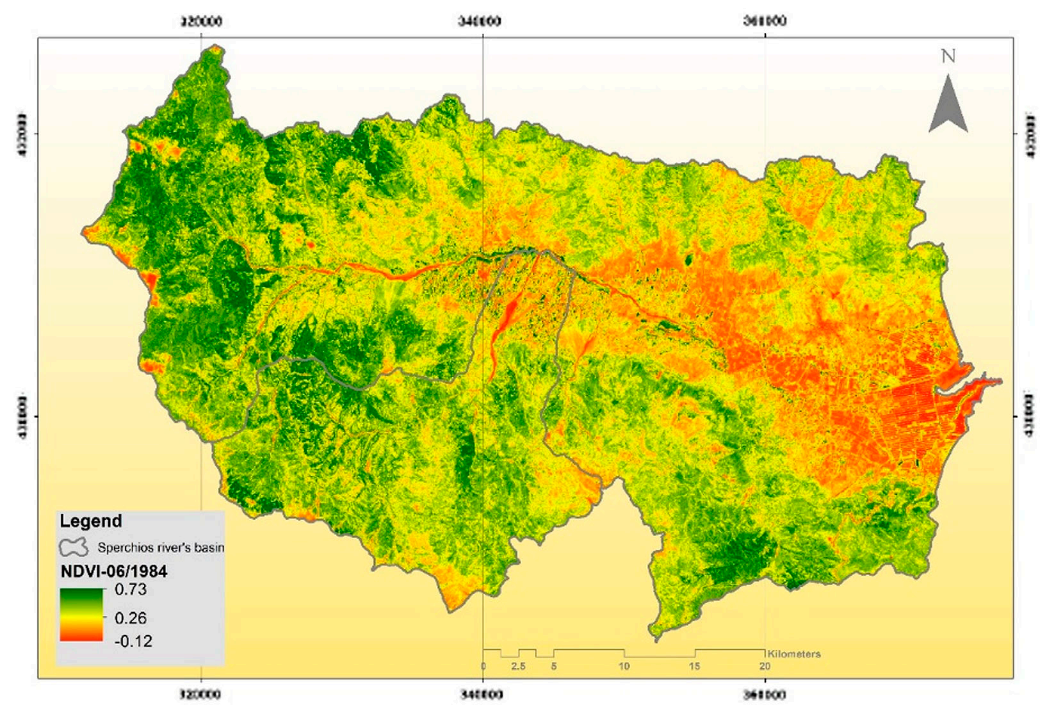

Fig. 3. NDVI of Sperchios river's basin in 1984.

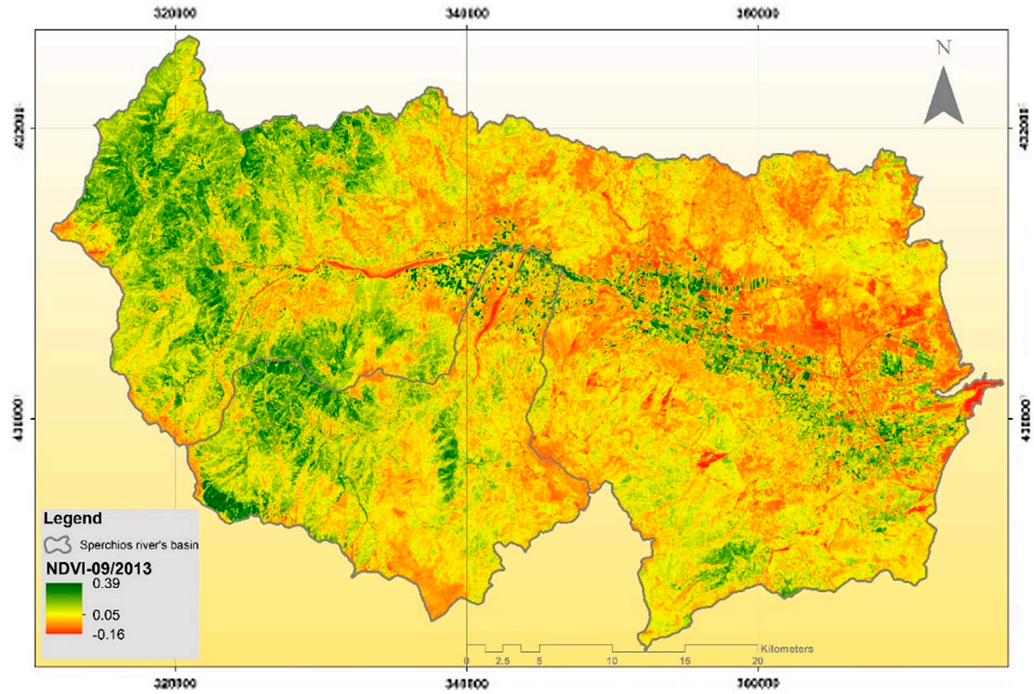

Fig. 4. NDVI of Sperchios river's basin in 2013.

detected in NDVIs of 1984–2013. The majority of 1984 NDVI data is lower than –0.25, whereas some extreme NDVI values of 2013 are presented higher than –0.25 (Fig. 6). Since negative NDVI values greater than –0.1 have trivial ecological meaning, it was decided to exclude them from the mapping of the NDVIs.

Higher NDVI values of 1972–1984 can be attributed partially to the climatic conditions that have been favourable for vegetation growth in the 1990s compared to 2013, the great increase in the area of heath land from 1972 to 2013 as it will be accrued from the land use classification results and ultimately to the different dates of satellite images (09/1972, 06/1984) associated not only with the different phenological stage of vegetation, but also with the soil moisture.

Mean percentage NDVI change of Sperchios river basin is –84%, indicating an overall significant vegetation decrease (Fig. 7). The spatial distribution of the vegetation changes indicates significant and moderate decrease in almost whole basin with some exceptions along the Sperchios river where the vegetation is slightly decreased. More particular, vegetation decrease coincides with the areas covered by forests, pastures and agricultural land while there is the possibility of replacement of some of the crops of 1972 with others in 2013. On the other hand, areas with vegetation increase are mainly located along the Sperchios river and at some regions north-western and south-western of the basin.

Combining the above-mentioned fluctuations with the regional topography, it becomes evident that the regions that present decreased vegetation are mountainous, unexploited and situated at high altitude (900–2,400 m), whereas regions with medium decreased vegetation during 1972–2013 are lowlands (0–500 m), dominated by urban areas and agricultural lands.

The frequency distribution and box-plots diagrams of NDVI (Figs. 5 and 6) illustrate the significant decreasing trend of the vegetation cover in the study area. This trend is not linear since in 1984 higher and more dispersed values of NDVI are observed, but this may be due to the slightly different date of the satellite images (September in 1972–2013 while June in 1984). Nevertheless, in 1972, 50% of the area (between 25th and 75th percentiles) have NDVI values between 0.14 and 0.28 while the respective values for 2013 are 0–0.9 (Table 1, Fig. 6). This clearly indicates a significant dropdown of the vegetation cover at a catchment scale, during the study period, as mentioned above.

3.2. Land use mapping and associated changes

The studied catchment area is dominated by forests that include coniferous, deciduous, evergreen-broadleaf and mixed forests, while they are mainly located at the northern, southern and western parts of

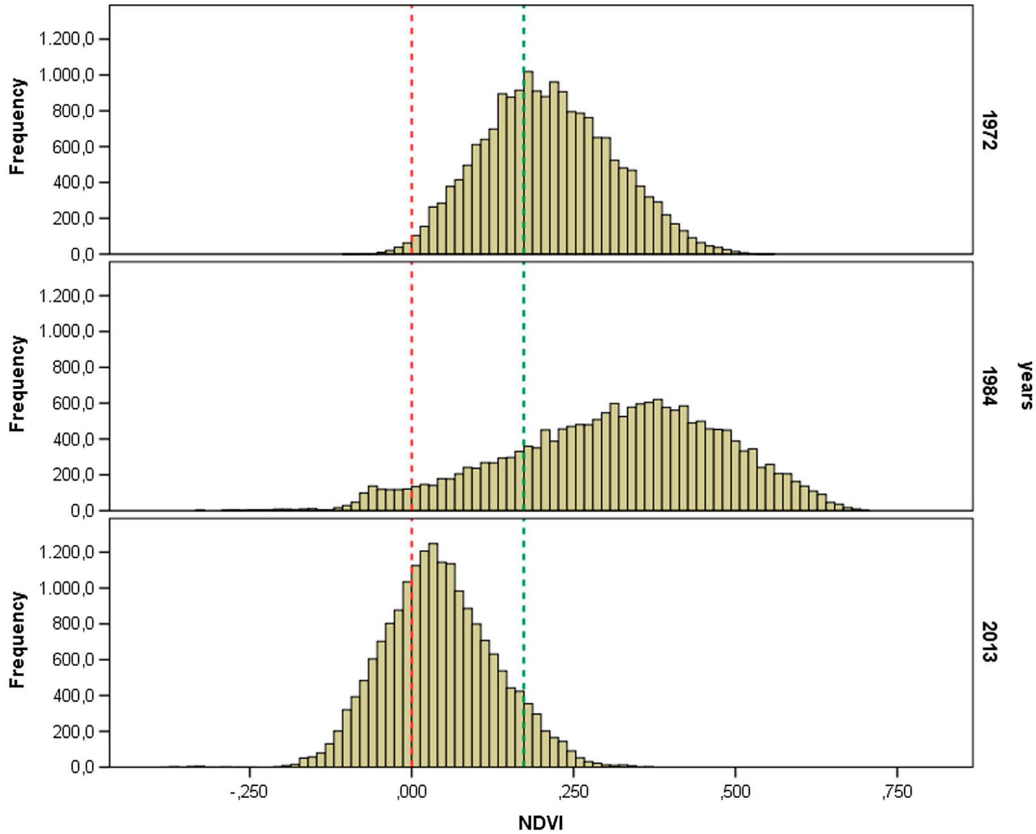

Fig. 5. The frequency distribution of NDVI values in Sperchios river's basin in 1972, 1984, and 2013 (red line: zero point, green line: median value of all data).

the Sperchios river's basin. The second largest land use category is the heath land while agricultural land follows including summer arable crops, tree crops, olive groves and vineyards. In 1972, pastures and low vegetation areas are ranked fourth (Fig. 8), while in 2013 in same position unified bare and urban land is detected (Fig. 9). This category contains areas with no vegetation especially in summer and concern crops on fallow or abandoned fields, as well as continuous and discontinuous urban constructions (all artificial surfaces, roads and rivers wider than five measures as well as drainage and irrigation channels).

Conclusively, the temporal land use variation between the study periods 1972–2013 is mainly characterized by reduced forests and pastures by 28 and 26%, respectively, increased cultivations by 47%, increased heath land by 114% and decreased surface of bare and urban land 12%. Therefore, main land use changes indicate the conversion of some forest land to crops and heath land. These alterations can be attributed also to the significant changes of socio-economic conditions overall in Greece in the period 1972–2013 that concern the initial intensification and increment of agricultural activities and then the urbanization and abandonment of many rural areas. Subsequently, in order to validate the classification product, a comparison was conducted among the results of the present study and the study of [53], which regards the classification of satellite images Landsat 5 TM and Landsat seven ETM+.

Indicatively is stated that in 2007 forests cover an area of 1,018.9 km^2 [53] while in 2013 649.3 km^2 (this study), agricultural land [2007; 53] cover 458.3 km^2 while in 2013, 257 km^2 and in 2007 urban areas were approximately 87 km^2 [53]. Conclusively follows the inference that the land use changes' trends among the results are similar with emphasis to the major reduction of forests and natural vegetated areas.

The validation of the results indicated that classification accuracy reached the 75.4–85.2% for LULC of 1972–2013, respectively.

Then, the extent of each land cover was quantified for both of images and the descriptive statistics (Table 2) were performed, which revealed the long-term changes in the land cover during the past 40 years.

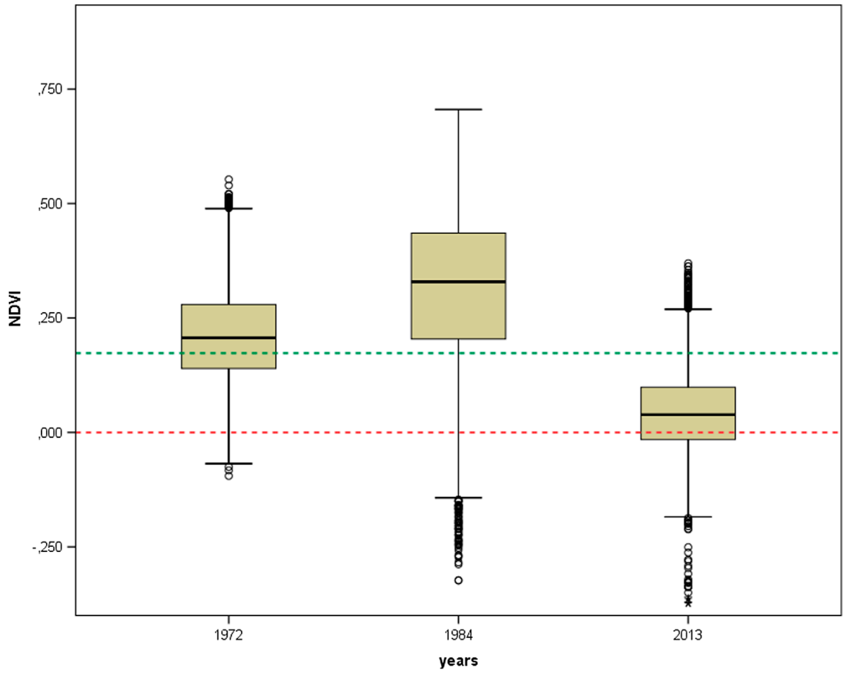

Fig. 6. Box plots representing NDVI values in Sperchios river's basin in 1972, 1984, and 2013 (red line: zero point, green line: median value of all data).

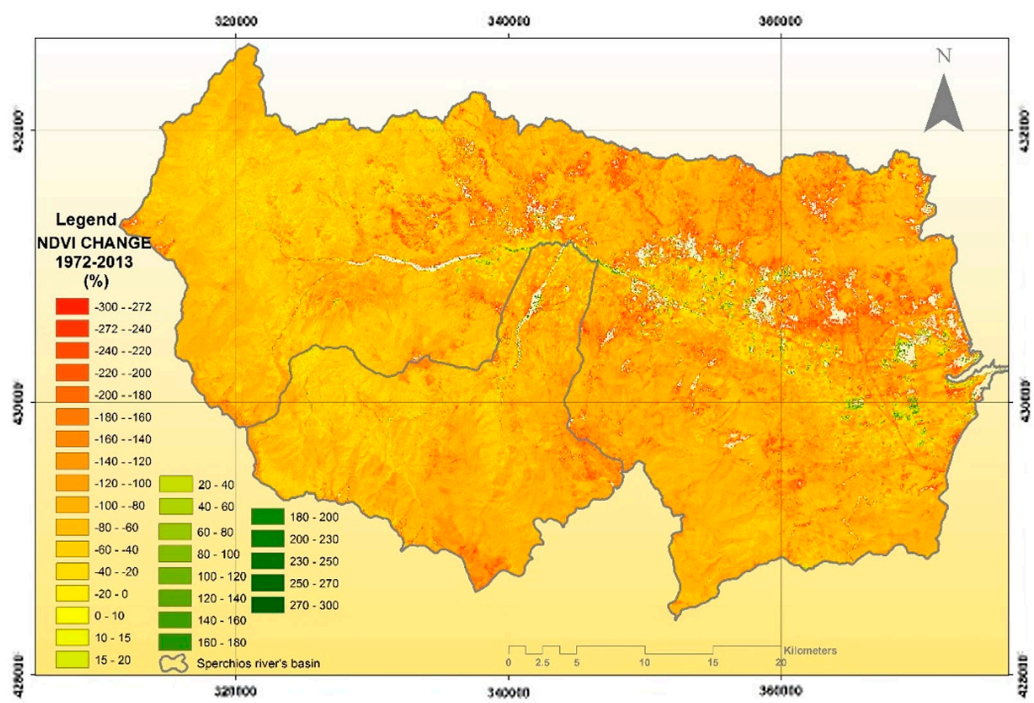

Fig. 7. Change in NDVI of Sperchios river's basin during 1972–2013.

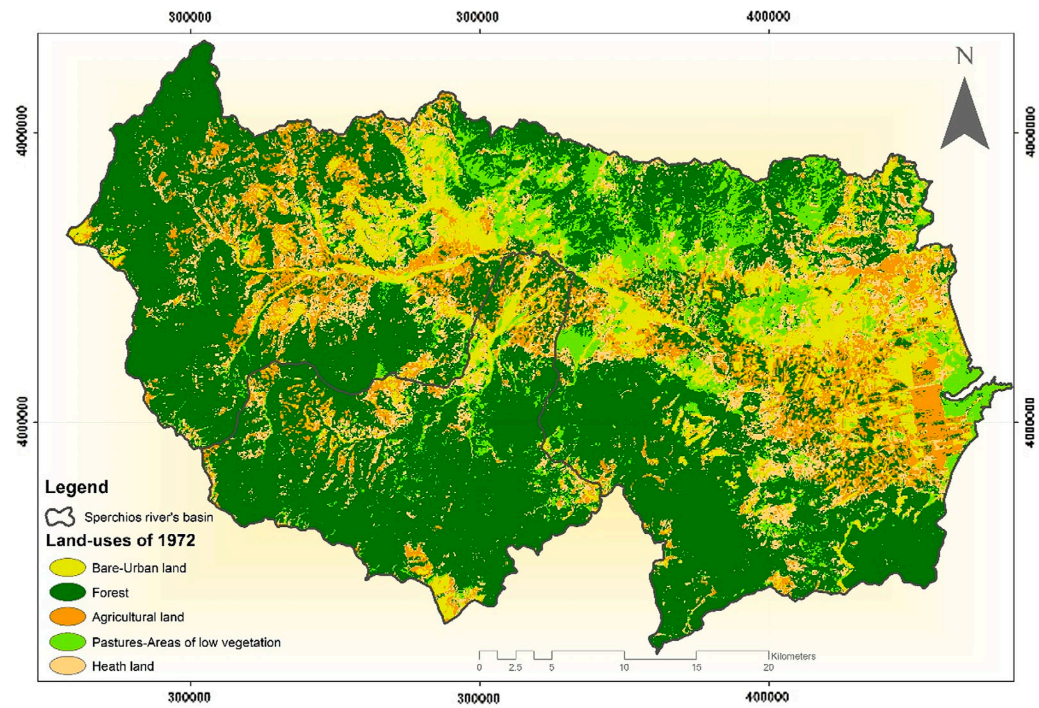

Fig. 8. Land use types of Sperchios river's basin in 1972.

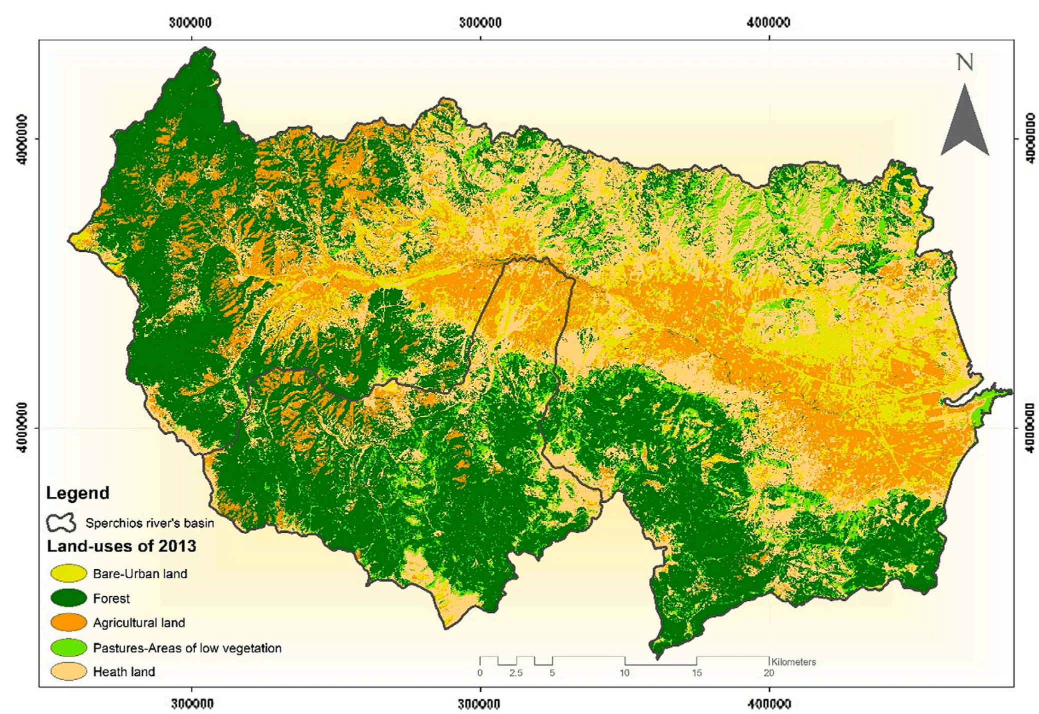

Fig. 9. Land use types of Sperchios river's basin in 2013.

Table 2
Land use types in the study area for the period 1972–2013 and the associated changes

Land use	1972 Area (km^2)	1972 (%)	2013 Area (km^2)	2013 (%)	Change (%) 1972–2013
Forests	900.8	57.3	649.3	41.6	−28
Pastures-low vegetated areas	161.2	10.3	119.3	7.7	−26
Heath land	190	12.1	407.3	26.1	+114
Agricultural land	174.7	11.1	256.99	16.5	+47
Bare-urban land	145.1	9.2	127.8	8.2	−12

4. Land use classification and challenges

During the land use classification process, some problems were encountered that made the achievement of high accuracy difficult by affecting the behaviour of the classification algorithm. The major problem, that strongly characterizes Greece, is the intense fragmentation and diversity of agricultural land and the small size of the agricultural parcels. This feature results not only in increased mixed interclass pixels but also between two different classes, making the classification algorithm unable to distinguish them.

Another classification obstacle is the spectral confusion due to the aspect and slope of areas covered by (a) sparse scrub—grassland and dense shrub vegetation, (b) crops and bare land, (c) bare soil, olive groves and urban areas. This confusion is observed mainly in areas with intense brightness (reflectance) and involvement of many different types of land use. In order to outdistance the above-mentioned issues and record reliable changes of cover/land use, similar and comparable land use categories were created for each year (1972, 2013). More specifically, the separation of some areas with low vegetation from pasture and areas with sparse or no vegetation from urban construction was particularly difficult, therefore it was preferred to unify these classes into one. Moreover, the applied classification algorithm on Landsat 5 TM (1984), resulted in different land use classes compared to others, hence according to the above-mentioned rationale, it was omitted from the classification procedure.

5. Discussion and conclusions

This article is an effort to quantify land use and vegetation changes in the Sperchios river's catchment from 1972 to 2013 since their assessment on hydrology is essential for the development of sustainable water resource strategies.

The obtained NDVI maps indicate that denser and more abundant vegetation dominates in medium and high elevated areas where coniferous, transitional and broad-leaved forests are detected, whereas areas covered by bare-urban land and pastures present lower NDVI values.

The temporal trends of NDVI indicate that vegetation density increases, during the aforementioned period, in areas that are mainly located along the Sperchios river and at some regions north-western and south-western of the basin, whereas the vegetation density and coverage decrease coincides with the areas covered by forests, pastures and agricultural land. Likewise there is the possibility of replacement of some of the crops of 1972 with others in 2013.

Thereafter, satellite imagery classification was implemented and a land use classification algorithm was applied to map the relevant changes from 1972 to 2013.

These results indicate that the decrease of forests and pastures led to the increase of agricultural and heath land. Both bare and urban land covers have moderately been decreased during the study period.

Landsat time series analysis have been proven to be useful in order to get the vegetation and LULC changes information while NDVI of two images analysis is more detailed information to combine with land use/cover change condition in the interest of getting the vegetation density distribution. More research is needed about the higher land use classification accuracy of Landsat 8 OLI image than Landsat 1 MSS and the different classification results of Landsat 5 TM image.

This research study has been carried out in the context of the KRIPIS research project with the view of development of methodologies for integrated river basin management and associated coastal and marine zone and study areas the Sperchios river and Maliakos Gulf (Greece). This preliminary stage intends to contribute to overall ecological quality assessment of Sperchios river by incorporating remotely sensed data into hydraulic and ecological simulation models of Sperchios river's basin.

Aknowledgements

This work have been funded by the Hellenic General Secretariat of Research and Technology, under the KRIPIS framework program with title: "Development of an integrated management scheme combining both catchment and coastal/sea zones", ESPA 2007–2013.

References

[1] C. Chen, C.R. Chen, N. Son, Investigating rice cropping practices and growing areas from modis data using empirical mode decomposition and support vector machines, GISci. Remote Sens. 49 (2012) 117–138.
[2] K.M. de Beurs, G.M. Henebry, Land surface phenology, climatic variation, and institutional change: Analyzing agricultural land cover change in Kazakhstan, Remote Sens. Environ. 89(4) (2004) 497–509.
[3] E.P. Glenn, A.R. Huete, P.L. Nagler, S.G. Nelson, Relationship between remotely-sensed vegetation Indices, canopy attributes and plant physiological processes: What Vegetation indices can and cannot tell us about the landscape, Sensors 8 (2008) 2136–2160.
[4] P. Gong, J. Wang, L. Yu, Y.C. Zhao, Y.Y. Zhao, L. Liang, Z.G. Niu, X.M. Huang, H.H. Fu, S. Liu, C.C. Li, X.Y. Li, W. Fu, C.X. Liu, Y. Xu, X.Y. Wang, Q. Cheng, L.Y. Hu, W.B. Yao, H. Zhang, P. Zhu, Z.Y. Zhao, H.Y. Zhang, Y.M. Zheng, L.Y. Ji, Y.W. Zhang, H. Chen, A. Yan, J.H. Guo, L. Wang, X.J. Liu, T.T. Shi, M.H. Zhu, Y.L. Chen, G.W. Yang, P. Tang, B. Xu, C. Giri, N. Clinton, Z.L. Zhu, J. Chen, J. Chen, Finer resolution observation and monitoring of global land cover: First mapping results with Landsat TM and ETM+ data, Int. J. Remote Sens. 34 (2013) 2607–2654.
[5] J. Lambert, C. Drenou, J. Denux, G. Balent, V. Cheret, Monitoring forest decline through remote sensing time series analysis, GISci. Remote Sens. 50 (2013) 437–457.
[6] S. Bhatti, N. Tripathi, Built-up area extraction using Landsat 8 OLI imagery, GIScience & Remote Sensing 51 (2014) 445–467.
[7] J. Im, Z. Lu, J. Rhee, J.R. Jensen, Fusion of feature selection and optimized immune networks for hyperspectral image classification of urban landscapes, Geocarto Int. 27 (2012) 373–393.
[8] W. Kleynhans, J.C. Olivier, K.J. Wessels, B.P. Salmon, F. van den Bergh, K. Steenkamp, Detecting land cover change using an extended Kalman filter on MODIS NDVI time-series data, IEEE Geosci. Remote Sens. Lett. 8(3) (2011) 507–511.
[9] Y. Liu, X. Wang, H. Tani, N. Matsuoka, S. Matsumura, Spatial and temporal relationships among NDVI, climate factors, and land cover changes in Northeast Asia from 1982 to 2009, GISci. Remote Sens. 48 (2011) 371–393.
[10] R.S. Lunetta, J.F. Knight, J. Ediriwickrema, J.G. Lyon, L.D. Worthy, Land-cover change detection using multi-temporal MODIS NDVI data, Remote Sens. Environ. 105(2) (2006) 142–154.
[11] V. Chéret, J. Denux, Analysis of MODIS NDVI time series to calculate indicators of mediterranean forest fire susceptibility, GISci. Remote Sens. 48 (2011) 171–194.
[12] J.U. Hielkema, S.D. Prince, W.L. Astle, rainfall and vegetation monitoring in the savanna zone of the Democratic Republic of Sudan using the noaa advanced very high resolution radiometer, Int. J. Remote Sens. 7(11) (1986) 1499–1513.
[13] J. Im, Z. Lu, J. Rhee, J.R. Jensen, Fusion of feature selection and optimized immune networks for hyperspectral image classification of urban landscapes, Geocarto Int. 27 (2012) 373–393.
[14] M. Li, J. Im, C. Beier, Machine learning approaches for forest classification and change analysis using multi-temporal Landsat TM images over huntington wildlife forest, GISci. Remote Sens. 50(4) (2013) 361–384.
[15] Q. Meng, W. Cooke, J. Rodgers, Derivation of 16-day time-series NDVI data for environmental studies using a data assimilation approach, GISci. Remote Sens. 50 (2013) 500–514.
[16] I. Ozdemir, Linear transformation to minimize the effects of variability in understory to estimate percent tree canopy cover using RapidEye data, GISci. Remote Sens. 51 (2014) 288–300.
[17] F. Yuan, C. Wang, M. Mitchell, Spatial patterns of land surface phenology relative to monthly climate variations: US Great Plains, GISci. Remote Sens. 51 (2014) 30–50.
[18] X. Zhang, M.A. Friedl, C.B. Schaaf, A.H. Strahler, J.C. Hodges, F. Gao, B.C. Reed, A. Huete, Monitoring vegetation phenology using MODIS, Remote Sens. Environ. 84(3) (2003) 471–475.
[19] J. Peng, Z. Liu, Y. Liu, J. Wu, Y. Han, Trend analysis of vegetation dynamics in qinghai-tibet plateau using hurst exponent, Ecol. Ind. 14 (2012) 28–39.
[20] Z.M. Zhang, F.V. Coillie, E.M. De Clercq, X. Ou, R. De Wulf, Mountain vegetation change quantification using surface landscape metrics in Lancang watershed, China, Ecol. Ind. 31 (2013) 49–58.
[21] C.J. Tucker, J.R.G. Townshend, T.E. Goff, African land-cover classification using satellite data, Science 227 (1985) 369–375.
[22] K. Jia, Q.Z. Li, Y.C. Tian, B.F. Wu, F.F. Zhang, J.H. Meng, Crop classification using multi-configuration SAR data in the North China plain, Int. J. Remote Sens. 33 (2012) 170–183.
[23] J.R. Townshend, J.G. Masek, C.Q. Huang, E.F. Vermote, F. Gao, S. Channan, J.O. Sexton, M. Feng, R. Narasimhan, D. Kim, K. Song, D.X. Song, X.P. Song, P. Noojipady, B. Tan, M.X. Li, R.E. Wolfe, Global characterization andmonitoring of forest cover using Landsat data: Opportunities and challenges, Int. J. Digital Earth 5 (2012) 373–397.
[24] V. Markogianni, E. Dimitriou, D.P. Kalivas, Land-use and vegetation change detection in Plastira artificial lake catchment (Greece) by using remote-sensing and GIS techniques, Int. J. Remote Sens. 34(4) (2013) 1265–1281.
[25] C.Q. Huang, K. Song, S. Kim, J.R.G. Townshend, P. Davis, J.G. Masek, S.N. Goward, Use of a dark object concept and support vector machines to automate forest cover change analysis, Remote Sens. Environ. 112 (2008) 970–985.
[26] M. Shimada, O. Isoguchi, T. Motooka, T. Shiraishi, A. Mukaida, H. Okumura, T. Otaki, T. Itoh, Generation of 10 m resolution PALSAR and JERS-SAR mosaic andforest/non-forest maps for forest carbon tracking,

in: 2011 IEEE International Geoscience and Remote Sensing Symposium, IEEE Press, Vancouver, Canada, 2011, pp. 3510–3513.
[27] USGS, Relation of Benthic Macro-Invertebrate Community Impairment to Basin Characteristics in New Jersey Streams, National Water Quality Assessment Program Long unit-New Jersey, New Jersey, NJ, 1998.
[28] D.N. Wear, M.G. Turner, R.J. Naiman, Land cover along an urban-rural gradient: Implications for water quality, Ecol. Appl. 8 (1998) 619–630.
[29] R.A. Zampella, N.A. Procopio, Landscape Patterns and Water-Quality Relationships in New Jersey Pinelands Streams, Pinelands Commission, New Jersey, NJ, 2009.
[30] W.B. Meyer, L. Turner, Changes in Land Use and Land Cover: A Global Perspective, Cambridge University Press, Cambridge England, New York, NY, 1994.
[31] GLP, Science Plan and Implementation Strategy, IGBP Secretariat, Global Land Project (GLP), Stockholm, 2005.
[32] R.A. James, E.H. Ernest, T. John, A Landuse and Land Cover Classification System for Use With Remote Sensor Data, Geology Survey Professional Paper, UN Government Printing Office, Washington, DC, 1995.
[33] FAO, Control of Water Pollution from Agriculture, FAO Corporate Document Repository, Canada, 1996.
[34] S. Schock, Projecting Land-Use Change: A Summary of Models for Assessing the Effects of Community Growth and Change on Land-Use Patterns, US Environmental Protection Agency, Washington, DC, 2000.
[35] D.R. Lenat, J.K. Crawford, Effects of landuse on water quality and aquatic biota of three North Carolina Piedmont streams, Hydrobiologia 294 (1994) 185–199.
[36] E. Erle, P. Robert, Land-use and land-cover change, in: Encyclopedia of Earth Cutler J. Cleveland: Environmental Information Coalition, National Council for Science and the Environment, Washington, DC, 2010.
[37] R.A. Young, C.A. Onstad, D.D. Bosch, W.P. Anderson, A nonpoint-source pollution model for evaluating agricultural watersheds, Soil Water Conserv. 44(2) (1989) 168–173.
[38] M. Feng, C. Huang, S. Channan, E.F. Vermote, J.G. Masek, J.R. Townshend, Quality assessment of Landsat surface reflectance products using MODIS data, Comput. Geosci. 38(1) (2012) 9–22.
[39] J. Ju, D. Roy, E. Vermote, J. Masek, V. Kovalskyy, Continental-scale validation of MODIS-based and LEDAPS Landsat ETM+ atmospheric correction methods, Remote Sens. Environ. 122 (2012) 175–184.
[40] T.K. Maiersperger, P.L. Scaramuzza, L. Leigh, S. Shrestha, K.P. Gallo, C.B. Jenkerson, J.L. Dwyer, Characterizing LEDAPS surface reflectance products by comparisons with AERONET, field spectrometer, and MODIS data, Remote Sens. Environ. 136 (2013) 1–13.
[41] G. Efthimiou, A. Mertzanis, M. Sapountzis, G. Zakynthinos, Anthropogenic effects on Spercheios river Delta. Actions for Protection, Distinction and Management of Natural Ecosystems, International Conference for Environmental Technology—"Heleco '05" Athens, Greece, 2005.
[42] G. Efthimiou, C. Topaloglou, S. Monachou, K. Kaprana, Change detection in Natura 2000 area of Spercheios river in central Greece using remote sensing and GIS, J. Int. Sci. Publ. Ecol. Saf. 8 (2014) 259–259.
[43] D. Koutsogiannis, G. Tsakalias, Hydrological characteristics of Spercheios Basin, Spercheios 2000+ Environment and Development, Lamia, Greece, 1995.
[44] A. Zamani, H. Maroukian, Deltaic sedimentation of the Sperchios River in historical times, Ann. Geologiques du Pays Helleniques 30 (1980) 430–440.
[45] A. Mertzanis, F.M. Maceo, G. Angeli, A. Stanica, A. Galvani, P. Gasparetto, F. Pontoni, Sediment Transport and Geomorphological Evolution in River Systems & Coastal Zones in Italy, Romania and Greece, Giraldi ed., Atti den Convegno Italy-China: An Ancient Cultural Heritage and the Challenge for Future Development, Bologna, Italy, 2012.
[46] YCEO - Yale Center for Earth Observation, Yale Institute of Biospheric Studies, Index of CEO Documentation, 2010. Available From: <http://www.yale.edu/ceo/Documentation/>.
[47] L.E. Keiner, X. Yan, A neural network model for estimating sea surface chlorophyll and sediments from thematic mapper imagery, Remote Sens. Environ. 66 (1998) 153–165.
[48] R.G. Lathrop, T.M. Lillesand, B.S. Yandell, Testing the utility of simple multi-date Thematic Mapper calibration algorithms for monitoring turbid inland waters, Int. J. Remote Sens. 12 (1991) 2045–2063.
[49] T.M. Lillesand, R.W. Kiefer, Remote Sensing and Image Interpretation, third ed., John Wiley & Sons, Inc., New York–Chichester–Brisbane–Toronto–Singapore, 1994, pp. 750, ISBN: 0-471-57783-9.
[50] K.S. Han, J.-L. Champeaux, J.L. Roujean, A land cover classification product over France at 1 km resolution using SPOT4/VEGETATION data, Remote Sens. Environ. 92 (2004) 52–66.
[51] K.R. Zalik, An efficient k-means clustering algorithm, Pattern Recognit. Lett. 29(9) (2008) 1385–1391, doi: 10.1016/j.patrec.2008.02.014.
[52] P. Riloki, S. Dharmendra, S. Tanuja, Advanced fractal approach for unsupervised classification of SAR images, Adv. Space Res. Interfaces 45 (2010) 1338–1349.
[53] E. Psomiadis, Research of the geomorphological and environmental changes in the hydro- logical basin of Sperchios River by using new techniques, PhD thesis, Agricultural University of Athens, Athens, 2010.
[54] L. Gass, L.M. Norman, M.L. Villarreal, C. Tolle, M. Coe, P. Jamwal, A Test of Methods to Measure Vegetation Change Adjacent to Gabions in Sonora, Mexico using Landsat imagery, Presented at the Santa Cruz River Researcher's Day, Tucson, Arizona, 2013.